Manuscript prepared for Atmos. Chem. Phys. Discuss.
with version 2015/04/24 7.83 Copernicus papers of the LaTeX class copernicus.cls.
Date: 23 October 2015

Global and zonal tropospheric ozone variations from 2003–2011 as seen by SCIAMACHY

F. Ebojie[1], J. P. Burrows[1], C. Gebhardt[1], A. Ladstätter-Weißenmayer[1], C. von Savigny[2], A. Rozanov[1], M. Weber[1], and H. Bovensmann[1]

[1]Institute of Environmental Physics (IUP), University of Bremen, P.O. Box 330440, 28334 Bremen, Germany
[2]Institute of Physics, Ernst-Moritz-Arndt-University of Greifswald, Felix-Hausdorff-Str. 6, 17489 Greifswald, Germany

Correspondence to: F. Ebojie (felix@iup.physik.uni-bremen.de)

Abstract

An analysis of the tropospheric ozone (O_3) columns (TOCs) derived from SCIAMACHY limb-nadir-matching (LNM) observations during 2003–2011, focusing on the zonal and global variations in TOC is described. Trends changes are derived using a multivariate linear regression model. TOC shows a change of $-0.2\pm0.4\,\%\,yr^{-1}$, $0.3\pm0.4\,\%\,yr^{-1}$, $0.1\pm0.5\,\%\,yr^{-1}$ and $0.1\pm0.2\,\%\,yr^{-1}$, which are not statistically significant at the $2\,\sigma$ level in the latitude bands 30–50° N, 20° S–0, 0–20° N and 50–30° S, respectively. Tropospheric O_3 shows statistically significant increases over some regions of South Asia (1–3 $\%\,yr^{-1}$), the South American continent (up to 2 $\%\,yr^{-1}$), Alaska (up to 2 $\%\,yr^{-1}$) and around Congo in Africa (up to 2 $\%\,yr^{-1}$). Significant increase in TOC is derived from the continental outflows including those of Australia (up to 2 $\%\,yr^{-1}$), Eurasia (1–3 $\%\,yr^{-1}$) and the South America (up to 3 $\%\,yr^{-1}$). Significant decrease in TOC (up to $-3\,\%\,yr^{-1}$) is observed over some regions of the continents of North America, Europe and South America. Over the Oceanic regions, significant decrease in TOC of about $-2\,\%\,yr^{-1}$ is observed over the outflows of Europe and North America.

1 Introduction

Tropospheric ozone (O_3) is a major environmental concern. The amount of tropospheric O_3 has been shown to be increasing globally during the 20th century due to enhanced emissions of anthropogenic precursors (Marenco et al., 1994; Shindell et al., 2006). Tropospheric O_3 is an important greenhouse gas and a pollutant. It affects air quality and contributes to global warming (e.g., Shindell et al., 2006; Jacob and Winner, 2009). It is responsible for respiratory diseases in humans and causes damage to crops and ecosystems (e.g., Lippmann, 1991; Jacobson, 2012). Ozone is a strong oxidant and a precursor of hydroxyl (OH) and hydroperoxy (HO_2) radicals, which drive tropospheric chemistry (Levy, 1971; Logan et al., 1981). Tropospheric O_3 has two main sources: photochemical production within the troposphere and transport from the stratosphere. The photochemical source

of tropospheric O_3 is mainly controlled by emissions of O_3 precursors including nitrogen oxides (NO_x) and volatile organic compounds (VOCs) (Hao and Wang, 1952; Lelieveld and Dentener, 2000). Instantaneous rates of formation of O_3 are dependent on the relation between O_3, NO_x and VOC from which two regimes with different O_3-NO_x-VOC sensitivity can be identified, i.e. a NO_x-sensitive regime (limited NO_x and high VOC) and a VOC-sensitive regime (saturated NO_x and low VOC). In the NO_x-sensitive regime, O_3 concentrations increase with increasing NO_x and exhibit little response to increasing VOC. In the VOC-sensitive regime, O_3 concentrations decrease with increasing NO_x and increase with increasing VOC. While the NO_x-sensitive regime is associated with high VOC/NO_x ratios, the VOC-sensitive regime is associated with low VOC/NO_x ratios. The O_3-NO_x-VOC sensitivity varies with location, events and time. The VOC-sensitive chemistry is more likely in the urban area or pollution source region, while the NO_x-sensitive chemistry is more likely downwind (Milford et al., 1989; Duncan et al., 2010). O_3 precursors such as NO_x and VOCs are emitted from fossil fuel combustion, power plants, biomass burning, lightning and other combustion sources. They are also emitted from microbes in the soil and from vegetation (Guenther et al., 2000). High amounts of O_3 precursors anthropogenically produced can accumulate to a hazardous level during favourable meteorological conditions (Zhang et al., 1998). The reaction of carbon monoxide (CO), VOCs, and methane (CH_4) with OH radicals is the main source of peroxy (RO_2, HO_2) radicals, which facilitate the conversion of nitric oxide (NO) to nitrogen dioxide (NO_2). Hence, a decrease in the chemical fuels (CO, VOCs, CH_4) may ultimately lead to a decrease in the production of NO_2. Increase in tropospheric NO_x concentrations can lead to increase in O_3. However under conditions of high NO_x (reaching to levels beyond 10 ppb), which are found mainly in pollution source regions in some urban centers and around power plants, O_3 can be lost or titrated via the reaction: $NO + O_3 \rightarrow NO_2 + O_2$ (e.g., Sillman et al., 1990; Brasseur et al., 1999). Nevertheless, O_3 is reformed downwind in the plume from the urban area (e.g., Crutzen, 1979). The influx of O_3-rich stratospheric air through stratosphere-troposphere exchange (STE) also contributes to tropospheric O_3 abundance. O_3 is transported from the lower stratosphere into the upper troposphere through tropopause foldings (Danielsen, 1968; Fusco and Logan,

2003) and it is exchanged with the troposphere via diabatic processes and turbulent diffusion (Lamarque and Hess, 1994), mixing processes and convective injection during the breakup of stratospheric filaments (e.g., Appenzeller et al., 1996).

Chemical removal of tropospheric O_3 occurs by photolysis and catalytic reactions involving hydrogen and oxides of hydrogen ($OH + HO_2$) as well as halogen and halogen oxides (Finlayson-Pitts et al., 1990; Monks, 2005; Gentner et al., 2014). In addition, O_3 oxidizes VOCs with double bonds (e.g., isoprene, methanol, acetone, etc.) and is also removed from the troposphere by deposition to the surface. The photolysis of O_3 plays a [illegible] role in tropospheric chemistry and it is strongly determined by the stratospheric O_3 columns. It has been observed that a negative trend in stratospheric O_3 enhances the O_3 photolysis in the troposphere as a result of increasing UV-B radiation (WMO, 1999). The combination of sources, loss processes and transport within the troposphere determines the amount of O_3 at any given time and location within the troposphere i.e., its spatial and temporal distribution and variability.

The factors contributing to trends in background O_3 include changes in emissions of O_3 precursors, meteorological variability (changes in temperature and solar radiation), and regional and intercontinental transport of O_3 and its precursors (Jacob et al., 1999; Liu et al., 2002). Changes in circulation and stratospheric ozone intrusions also play a role (e.g., Dickerson et al., 1995; Cooper and Parrish, 2004). Furthermore, interannual to decadal climate variability can also contribute to changes in ozone.

In the 20th century, the annual mean concentrations of tropospheric O_3 at the northern mid and high latitudes were found to have more than doubled (Marenco et al., 1994; Shindell et al., 2006). Although O_3 mitigation efforts in the developed countries have led to a decrease in peak O_3 levels in both urban and rural areas and led to negative trends on a regional scale, particularly over Europe and North America in recent years (Naja et al., 2003; Derwent et al., 2003; Cooper et al., 2014; Parrish et al., 2013, 2014), background levels continue to increase in some regions (Oltmans et al., 2006). Furthermore, O_3 concentrations over some developed and developing countries are rising due to increased emissions of NO_x and other O_3 precursors from anthropogenic activities (e.g., Dentener et al., 2005).

As a result of regional and intercontinental transport of O_3 (e.g., Fiore et al., 2009; Parrish et al., 1993), increase in O_3 is not only limited to local/regional sources but also hemispheric scale sources (TOR-2, 2003).

Trends in tropospheric O_3 have been derived from measurements from urban and rural sites (e.g., Oltmans et al., 2006, 2013; Cooper et al., 2012), ozonesondes and commercial aircraft (e.g., Logan et al., 2012). Ozone trends derived from satellite measurements have been published (e.g., Ziemke et al., 2005; Beig and Singh, 2007). Some of the TOC trends based on satellite measurements are derived from different instruments with differing algorithms and sampling characteristics and this can introduce some uncertainties in the data sets (Beig and Singh, 2007; Doughty et al., 2011). Most of the past tropospheric O_3 trend studies focused on regional pollution in the Northern Hemisphere (NH), where O_3 precursors are well characterized (e.g., Logan et al., 2012; Parrish et al., 2012). The goal of this study is to determine the zonal and global changes in the tropospheric O_3 data product derived from SCIAMACHY limb-nadir-matching (LNM) observations during the period 2003–2011. The manuscript is organized as follows: Sect. 2 briefly describes the data and regression model used in this study. Sect. 3 provides results and discussion, and Sect. 4 summarizes principal findings and conclusions.

2 Data and regression model

In this work, the tropospheric ozone column (TOC) time series derived from SCIAMACHY limb and nadir measurements for the period of 2003–2011 using the LNM technique (Ebojie et al., 2014; Ebojie, 2014), have been used to investigate their zonal and global linear trends. The LNM technique is a residual approach that subtracts stratospheric O_3 columns (SOCs), retrieved from the limb observations, from the total O_3 columns (TOZs), derived from the nadir observations. The technique requires accurate knowledge of the SOCs, TOZs, tropopause height, and their associated errors. The SOCs were determined from the stratospheric O_3 profiles retrieved in the Hartley and Chappuis bands of O_3 from SCIAMACHY limb scattering measurements. The TOZs were also derived from SCIAMACHY

measurements, but in this case from the nadir viewing mode using the Weighting Function Differential Optical Absorption Spectroscopy (WFDOAS) technique in the Huggins band of O_3. Since TOCs constitute only about 10 % of the TOZs, small errors associated with clouds might significantly affect the derived TOCs. Therefore, limb scenes that are contaminated with clouds and nadir measurements that have a cloud fraction of more than 0.1 were screened out. Detailed discussion of the LNM technique applied to the retrieval of TOC from SCIAMACHY, analysis, a sensitivity study and validation of the SCIAMACHY TOC are given in Ebojie (2014) and Ebojie et al. (2014). The SCIAMACHY TOCs show good agreement with TOCs derived from other satellite instruments (Ebojie et al., 2014; Ebojie, 2014). The comparison of SCIAMACHY TOCs with co-located ozonesonde measurements show agreement to within 3 DU (Dobson Units) on average (Ebojie et al., 2014; Ebojie, 2014).

The SCIAMACHY tropospheric O_3 changes are determined using a multivariate linear regression taking the autocorrelation of consecutive values into account. This helps to reduce the uncertainties on the TOC trends and gives a better understanding of what drives O_3 trends and variability. In addition, the monthly mean time series were used in order to reduce the auto-correlation in the residuals. The implemented approach is similar to that used for stratospheric O_3 trends and variability by Gebhardt et al. (2014). The regression model is expressed as:

$$Z_t = \mu + \omega t + S_t + R(t) + \epsilon(t), \tag{1}$$

where Z_t is the monthly mean tropospheric O_3 data, t is the month index (1–108), μ is the intercept, ϵ is the error term, ω, which is the gradient or slope, represents the trend. S_t is the seasonal component including annual, semi-annual and the 4 and 3 month terms as shown in Eq. (2).

$$S_t = \sum_{i=1}^{4} \left(\beta_{1i} \sin\left(\frac{2\pi i t}{12}\right) + \beta_{2i} \cos\left(\frac{2\pi i t}{12}\right) \right). \tag{2}$$

β_{1i} and β_{2i} are parameters, which are determined to fit the amplitude and phase of the oscillations (von Clarmann et al., 2010; Eckert et al., 2014). The harmonics (12, 6, 4, 3 month)

are used to represent seasonal changes (Weatherhead et al., 2000). The 12 and 6 months correspond to the annual and semi-annual cycles, respectively. The terms with 4 and 3 month periods help to improve the fit quality mostly when the cycle shape is not sinusoidal (Stiller et al., 2012). The combination of sine and cosine terms provide a flexible adjustment to any phase of the (semi-) annual variation. $R(t)$ represents additional terms including the quasi-biennial oscillation (QBO) and El Niño-Southern Oscillation (ENSO), which can be expressed as:

$$R(t) = m\mathrm{QBO}_{50}(t) + n\mathrm{QBO}_{70}(t) + x\left(\mathrm{N}_{34}(t) + \frac{\mathrm{d}\mathrm{N}_{34}(t)}{\mathrm{d}t}\Delta(t)\right). \quad (3)$$

The first and second terms of Eq. (3) are the QBO terms, while the last term corresponds to the ENSO term. The factors m, n and x represent their fit coefficients. The QBO indices of 50 and 70 denote the pressure level of the ~~proxy~~. The solar term is not included in the regression model because the residuals show no evidence of a missing solar-cycle component. The different contributions to the regression model are described in more detail in Sect. 2.1. The trend uncertainty is $1\,\sigma$, which is defined by the covariance matrix of regression coefficients. The trends and their uncertainties are presented in relative units of $\%\,\mathrm{yr}^{-1}$, i.e., percent per year relative to the mean value of the underlying time series. The reported changes in TOC are considered statistically significant at the 95 % confidence level if the absolute ratio of the trend to its uncertainty is greater than 2 (Tiao et al., 1990).

2.1 QBO and ENSO signatures in ozone

El Niño-Southern Oscillation (ENSO) and quasi-biennial oscillation (QBO) influence tropospheric O_3 through modula of the stratospheric circulation (e.g., Simpson et al., 2011; Baldwin et al., 2001), O_3 (e.g., Oman et al., 2013), and STE O_3 influx (e.g., Zeng and Pyle, 2005). QBO is characterized by alternating easterly and westerly wind regimes within a variable period of 2–3 years (Pascoe et al., 1948). The QBO directly modulates tropical upwelling through the thermal wind balance. Although the QBO is a tropical phenomenon, it influences the entire stratospheric flow by modulating the effects of extrat-

ropical waves. It regulates the upwelling branch of the Brewer–Dobson circulation (BDC) and leads to variation in O_3 volume mixing ratio (VMR) mostly at the altitudes of steep O_3 VMR gradient, which is found below and above the maximum in the vertical O_3 VMR profiles (Butchart et al., 2003). QBO has been identified to affect the troposphere indirectly through its effect on the polar vortex (e.g., Holton and Tan, 1980). It directly affects the tropical and extratropical troposphere through convective anomalies (Haigh et al., 2005; Neu et al., 2014). Evidence of a QBO signal in the tropical troposphere O_3 has been recorded from satellite and ozonesonde measurements (e.g., Chandra et al., 2002; Lee et al., 2010). QBO can also affect the troposphere through tropospheric eddies even in the absence of an anomalous polar vortex or tropical convection (e.g., Garfinkel and Hartmann, 2011). A downward propagating QBO O_3 signal has been found to extend to the mid-troposphere where the phase analysis of the temperature anomalies implies that the driving force is a zonal mean overturning circulation associated with thermal wind adjustment (Lee et al., 2010). In the present study, the 50 and 70 hpa Singapore (1° N, 140° E) winds (http://www.geo.fu-berlin.de/en/met/ag/strat/produkte/qbo/, last access: 28 April 2015) are used as fit proxies. They are smoothed by a 4 month running mean and used globally in the form of Eq. (4).

$$\mathrm{QBO}(t) = m\mathrm{QBO}_{50}(t) + n\mathrm{QBO}_{70}(t). \quad (4)$$

Another dominant driver of interannual tropospheric variability is ENSO with a varying period of 2–7 years and maximizes around late boreal autumn to late winter (Bjerknes, 1966). The response of tropospheric O_3 to ENSO has been demonstrated (Chandra et al., 1998; Ladstätter-Weißenmayer et al., 1999; Zeng and Pyle, 2005; Valks et al., 2014; Ziemke et al., 2014; Coldewey-Egbers et al., 2014). Response to circulation and convective changes during El Niño lead to decrease in TOC in the central and East Pacific and an increase in the West Pacific/Indonesia (Fujiwara et al., 1999; Thompson et al., 2001; Valks et al., 2014; Ziemke et al., 2014). Statistically significant signals consistent with anomalous vertical motions during ENSO have been observed from tropospheric O_3 profiles associated with the Southern Oscillation Index (SOI) (Lee et al., 2010). In this study, an ENSO proxy based on

the anomalies of the Niño 3.4 index (http://www.cpc.ncep.noaa.gov/data/indices/,last access: 30 April 2015) is employed to reveal ENSO signatures in tropospheric O_3 time series. The combined fit of the proxy and its time derivative accounts for the time lag as shown in Eq. (5).

$$\mathrm{ENSO}(t) = x\left(\mathrm{N}_{34}(t) + \frac{\mathrm{dN}_{34}(t)}{\mathrm{d}t}\Delta(t)\right), \tag{5}$$

where N_{34} is the ENSO proxy and $\Delta(t)$ is the time lag. Therefore, to account for the non-linearity of $\frac{\mathrm{dN}_{34}(t)}{\mathrm{d}t}$, the fit starting with a time lag of 2 months is repeated with the lagged proxy until the remaining time lag approaches zero.

3 Results and discussion

3.1 Global distribution of tropospheric O_3

Analysis of the global distribution of tropospheric O_3 is important for the understanding of recent changes in O_3 and its precursor emissions. The tropospheric O_3 distribution reflects a balance between local production and destruction as well as atmospheric transport. Figure 1 shows the seasonal distribution of the global tropospheric O_3 in DU retrieved from SCIAMACHY observations averaged over 2003–2011 for 5° latitude × 5° longitude bins. Seasonal averages of the TOC provide a good ~~agreement~~ between minimizing variability associated with shorter time period averages ~~while still~~ providing information on seasonal dependence of long-term O_3 changes (Ebojie, 2014).

In the tropics, TOC in the top left panel of Fig. 1 for December–February shows a characteristic tropospheric O_3 wave-one feature, which is persistent in the southern tropics with higher TOC values (> 40 DU) over the southern Atlantic tropics than the southern Pacific as reported elsewhere (e.g., Fishman et al., 1990; Ebojie, 2014). This feature is observed in all seasons and maximizes in September–November with tropospheric O_3 values greater than 40 DU as compared to TOC values of less than 30 DU over the southern Pacific (Ebojie,

2014). The wave-one pattern in TOC originates from different contributing factors including biomass burning and lightning in both Africa and South America, deep convection in the Pacific region coupled with vertical injection of low marine boundary layer tropospheric O_3 into the middle and upper troposphere (the large scale Walker Circulation) (e.g., Fishman et al., 1990; Chandra et al., 2003; Sauvage et al., 07b). In the top right panel of Fig. 1, which corresponds to TOC for June–August. Largest TOC values ($>$ 45 DU) occur in the NH extratropics with a corresponding enhancement of TOC values ($>$ 35 DU) in the tropical/subtropical southern Atlantic region. The high level of tropospheric O_3 during boreal summer is primarily photochemically produced from anthropogenic pollution, biogenic VOCs and NO_x. Pollution effects with sources from STE, biomass burning, lightning also play a role during this season of the year as reported by many sources (e.g., Pfister et al., 2008; Thompson et al., 2008; Chandra et al., 2004). During March–May, i.e., bottom left panel of Fig. 1, NH springtime TOC buildup is observed. The high tropospheric O_3 values ($>$ 45 DU) in the northern subtropics and mid-latitudes are associated primarily to STE processes, which assume an annual maximum in these zonal bands (e.g., Chandra et al., 2004). Also of importance to the enhancement of O_3 in these zonal bands are tropospheric O_3 production sources including lightning, combustion of fossil fuels, biomass burning and soil emissions (e.g., Pfister et al., 2008; Thompson et al., 2008). There is a shift in the seasonal cycle from summer maximum to spring/summer peak mostly over northern mid-latitudes which can be attributed to either response to emissions reduction over the region or an increase in springtime O_3 or both (Parrish et al., 2013; Cooper et al., 2014). In the bottom right panel of Fig. 1, corresponding to TOC for September–November. The high TOC values ($>$ 40 DU) that lie along a zonal band of approximately 30–50° S in the Southern Hemisphere (SH) are similar to the high values observed at the mid-latitudes in the NH during summer and spring. These seasonal enhancements in TOC are of dynamical origin caused by STE (e.g., de Laat et al., 2005).

3.2 Global wind distribution

A good knowledge of the global wind distribution is necessary for the interpretation of changes in global tropospheric O_3 as it reveals information on the continental outflow and intercontinental transport of O_3 pollution. Variation in wind speed and direction can favour tropospheric O_3 variability. Changes in tropospheric O_3 are not only a consequence of chemical reactions but are also greatly affected by tropospheric circulation. Figure 2 shows contour plots of the global distribution of the seasonal winds speed in $\mathrm{m\,s^{-1}}$ at 500 hPa averaged over the years 2003–2011, which is overlaid with arrows (in blue) depicting wind direction. The plots are based on the ECMWF (European Centre for Medium-Range Weather Forecasts) Reanalysis Interim (ERA-I) wind data for 1.5° latitude × 1.5° longitude bins regridded to 5° latitude × 10° longitude bins for better identification of the magnitude and direction of the wind. The plots show that in the free troposphere, the easterlies prevail in the tropics while westerlies prevail at the extratropical region. Low wind speeds of less than $9\,\mathrm{m\,s^{-1}}$ dominate the tropics with wind speed of less than $6\,\mathrm{m\,s^{-1}}$ observed across part of South America, the Atlantic Ocean, Africa, the Indian Ocean and the maritime southeast Asia region. This shows the manifestation of the ITCZ (Intertropical Convergence Zone, Trenberth et al., 2000).

In the top left panel of Fig. 2, which corresponds to the wind distribution for December–February, high wind speed greater than $24\,\mathrm{m\,s^{-1}}$ is observed over the North Atlantic and North Pacific Oceans. A corresponding high wind speed ~~appear~~ over the southern extratropics, mostly in the 40–60° S latitude bands. During boreal summer (June–August), which is shown in the top right panel of Fig. 2, large wind speed greater than $18\,\mathrm{m\,s^{-1}}$ is observed over the southern extratropics with the largest wind speed greater than $24\,\mathrm{m\,s^{-1}}$ occurring in the region 40–60° S and 0–100° E. Some localized areas of high wind speed appear over the North Atlantic and North Pacific around the Gulf of Alaska, which are produced by tropical cyclones. An asymmetry in the winter to summer variation between the two hemispheres is observed. The largest seasonal variations in wind speed occur in the NH oceans mostly over the northern Atlantic. In contrast, the winter to summer variation in wind speed over the

SH oceans is relatively small. The largest wind speeds greater than 24 $m\,s^{-1}$ appear at the southern extratropics at all seasons with corresponding large wind speed in the northern extratropics during boreal winter, spring and autumn. These bands of high wind speed are associated with mid-latitude winter storms (Romanski et al., 2014). Similar wind patterns are observed in both hemispheres of March–May and September–November as shown in the bottom left and right panels of Fig. 2, respectively. Sudden reversal or change in wind direction ~~are~~ observed in all seasons between 15° and 35° in both hemispheres. This shows the manifestation of subtropical highs, which have been observed to have shifted due to direct radiative forcing from greenhouse gases among other processes (e.g., Hudson, 2012).

The middle-upper tropospheric anticyclone due to the response to the thermal and orographic forcing of the Tibetan Plateau has great impact on the atmospheric circulation in the NH (e.g., Ye and Wu, 1998; Zhang et al., 2005). The trans-Pacific transport of Asian pollution can influence changes in O_3 over North America and the Oceanic region (e.g., Jaffe et al., 1999; Parrish et al., 2012; Cooper et al., 2014), variation in the trans-Atlantic transport of North American pollution can influence pollution over Europe as well as the Atlantic Oceanic region (e.g., Derwent et al., 1998; Logan et al., 2012), and trans-Eurasian transport of European pollution can influence changes in O_3 over Asia (e.g., Liu et al., 2002; Parrish et al., 2012). The vertical wind velocity in the middle troposphere plays a significant role in controlling the amount of O_3 in the lower troposphere (Kim and Newchurch, 1996). Analysis shows that the centers of high velocity potential are associated with convergent inflow winds. The convergence in the upper troposphere corresponds to divergence in the lower troposphere, which is associated with downward vertical motion at the mid-troposphere. On the opposite side, a low velocity results in a vertical upward motion in the troposphere. Centers of lower tropospheric convergence and upper tropospheric divergence over the equatorial western Pacific are characterized by strong upward velocity at the mid-troposphere with maximum upward velocity outside the equatorial regions. The equatorial eastern Pacific is associated with upper tropospheric convergence, lower tropospheric divergence, and mid-tropospheric downward vertical motion (Wang, 2005). These are consistent with Pacific

climate features of the western Pacific warm pool and the equatorial eastern Pacific cold tongue.

3.3 Zonal mean tropospheric O_3 changes

O_3 trends are caused by long-term changes in ~~either~~ chemistry or dynamics or both. Zonal mean time series of monthly averaged tropospheric O_3 over four latitude bands (50–30° S, 20° S–0, 0–20° N and 30–50° N) are displayed in Figs. 3–6 with the time labeling on the x axis corresponding to the first month of the year. The TOC time series (black) are overlaid with their fitting curves (blue) and linear term plus offset (hereinafter referred to as linear, (violet)) from the regression model. The fit residuals are shown below the TOC time series. The individual terms from the regression including the harmonics, QBO, linear and ENSO terms are shown in the panels below, respectively. The time series of the fit parameters are coloured differently, i.e., pink, green, orange, and brown representing the harmonic, QBO, linear and ENSO terms, respectively, while the overlaid time series in black represents the time series with all fit terms removed except the particular fit parameter. Good fit quality is obtained in all four latitude bands. The fit residuals are typically on the order of a few DU. The annual cycles make comparable contributions to the fitting curves in all four latitude bands.

The harmonic terms show high values during hemispheric spring and summer for Figs. 3 and 4, which correspond to 50–30° S and 30–50° N latitude bands, respectively. Figures 5 and 6 show TOC in the latitude bands 20° S–0 and 0–20° N, respectively. We separated the southern tropics from the northern tropics due to the seasonal shift in TOC distributions in the tropics also reported in other studies (e.g., Valks et al., 2014; Ziemke et al., 2014). In Fig. 5, the harmonic terms show high values mainly during austral spring/summer. The O_3 maxima observed in Fig. 5 during austral spring/summer can be attributed mainly to transport of pollution and photochemical production of O_3. The combination of emissions from extensive biomass burning and transport of upper tropospheric O_3 production from lightning NO_x, especially in the southern tropics can contribute to the observed O_3 maxima in the top panel of Fig. 5. Such tropospheric O_3 maxima have been observed during austral

spring/summer in some studies (e.g., Sauvage et al., 2007b; Randel and Thompson, 2011; Thompson et al., 2014; Ziemke et al., 2014; Ebojie et al., 2014; Ebojie, 2014). The QBO fit captures the interannual variability in the regression analysis better in Fig. 5 than in Fig. 6, while the reverse is the case for the ENSO fit. The tropospheric O_3 seasonal cycle in the tropical region is primarily governed by two processes: the seasonal migration of the ITCZ and the photochemical production of O_3 from biomass burning and lightning activity (Moxim and Levy II, 2000; Thompson et al., 2000). These processes lead to vertical layers with strongly enhanced O_3 volume mixing ratios and hence the TOCs. The O_3 maxima observed in the subtropics and midlatitudes of both hemispheres (top panels of Figs. 3 and 4) can be associated with the combination of transport of O_3 and its precursors, local or regional photochemical production of O_3 as well as stratospheric intrusion of O_3 rich air masses into the troposphere (Chandra et al., 2004; Stohl et al., 2007; Pfister et al., 2008). The intercontinental transport of O_3 and its precursors can also contribute to the observed changes in tropospheric O_3 (Wild and Akimoto, 2001; Stohl et al., 2007; Cooper et al., 2012). In the southern subtropics and midlatitudes, the influence of both stratospheric intrusion and emissions from biomass burning (e.g., Sauvage et al., 2006; Wai et al., 2014) play a key role in the observed O_3 maxima during austral spring in Fig. 3. The QBO fit does not capture a significant contribution of the interannual variability in the regression analysis as observed in Figs. 3 and 4. The possible ENSO contributions are better identified in Fig. 4 than in Fig. 3.

Table 1 shows the results of TOC changes, the mean values and standard deviation over some zonal bands. An insignificant increase in tropospheric O_3 of $0.1 \pm 0.2\,\%\,\mathrm{yr}^{-1}$ with a mean value of 30.4 ± 4.9 DU is observed in the 50–30° S latitude band (Fig. 3). This region is mainly over the ocean with less influence from land, hence the uniformity in O_3 distributions in this zonal band as observed in Figure 12 of (Ebojie et al., 2014) and in (Ebojie, 2014). The observed insignificant positive change in O_3 in this zonal band may be due to a larger contribution of the significant positive change in TOC over southern South America compared to the significant negative change or no trend over the oceans as shown in Fig. 7.

A statistically insignificant decrease in TOCs of $-0.2 \pm 0.4\,\%\,\mathrm{yr}^{-1}$ with a mean value of 39.0 ± 3.9 DU is observed between 30° N–50° N (Fig. 4). This zonal band is greatly influenced by land-sea contrast in tropospheric O_3 and anthropogenic activity. The observed insignificant decrease in TOC over this latitude band could be associated with stronger significant negative TOC changes over Europe and North America than the significant positive change over northern China as observed in Fig. 7. Similar negative trends in TOC have been observed in other studies (e.g., Parrish et al., 2012; Vestreng et al., 2009; Cooper et al., 2012, 2014).

In the 20° S–0 latitudes band (Fig. 5), an insignificant positive change in tropospheric O_3 of $0.3 \pm 0.4\,\%\,\mathrm{yr}^{-1}$ with a mean value of 27.5 ± 3.9 DU is observed. The insignificant positive change in ozone in this region may be a consequence of a larger contribution by significant positive change in TOC over southern Africa and northern Australia outflow compared to the small significant negative change in TOC or no trend over the Oceans. The significant positive changes observed over southern Africa and the North Australian outflow region as shown in Fig. 7 may be a result of changes in O_3 precursor emission from anthropogenic activities. Changes in atmospheric circulation and emissions from biomass burning may also have contributed to the observed positive change in O_3 in this latitude band (Randel and Thompson, 2011; Thompson et al., 2014). In the 0–20° N latitude band (Fig. 6), an insignificant change in tropospheric O_3 of $0.1 \pm 0.5\,\%\,\mathrm{yr}^{-1}$ with a mean value of 29.3 ± 2.7 DU is observed. The small positive trend in TOC over this region results from many small positive and negative trends, most of them are statistically insignificant as observed in Fig. 7.

3.4 Global and regional mean tropospheric O_3 changes

3.4.1 Changes in SCIAMACHY global tropospheric O_3 columns

The changes in tropospheric O_3 are complex and vary both regionally and globally. They are strongly influenced by changes in precursor emissions, temperature, humidity, convection, STE, and hemispheric transport patterns. Figures 7 and 8 show changes in SCIAMACHY

TOC derived from 2003–2011 for 5° latitude × 5° longitude bins in % yr^{-1} and DU yr^{-1}, respectively. The colour ranges from blue to red, representing negative to positive changes in TOCs from 2003–2011. The white coloured area represents places with no TOC data due to the applied data screening criteria described in Ebojie et al. (2014) and Ebojie (2014). In the determination of TOC from SCIAMACHY LNM, limb scenes that are contaminated with clouds and nadir measurements that have a cloud fraction of more than 0.1 were screened out (Ebojie et al., 2014; Ebojie, 2014). This makes it unlikely, although not impossible, that the derived trends may be significantly affected by possible changes in cloud parameters from 2003 to 2011. The errors of the derived changes in TOCs are estimated at 1-sigma expressed in units of % yr^{-1} and DU yr^{-1}. The regions marked with cross signs represent changes in tropospheric O_3 significant at the 95 % confidence level.

Changes in TOC are observed along the outflow from continents to oceanic regions. Statistically significant changes in tropospheric O_3 are observed over the regions of North America, Europe, South Asia, South America and regions of Africa. Significant changes in O_3 are also observed over the marine region including the Pacific Ocean, Indian Ocean and the Atlantic Ocean. Significant positive changes in O_3 are observed over North America, especially around Alaska (region A in Fig. 7, up to 2 % yr^{-1}), which may be attributed to changes in both transport of pollution and photochemical production of O_3 from natural and anthropogenic precursor emissions. Significant negative TOC changes (up to -3 % yr^{-1}) are observed over some parts of North America, South America and Europe (regions B, C, D and E in Figs. 7 and 8), which can be attributed to decrease in anthropogenic NO_x and VOCs emissions as well as reduction in other tropospheric O_3 precursors (e.g., Vestreng et al., 2009; Logan et al., 2012). Increase in anthropogenic and biogenic halogens may also play a role in the observed significant negative change in TOC over North America and Europe (von Glasow et al., 2002; Read et al., 2008). Similar significant negative trends in tropospheric O_3 have been observed in some earlier studies (e.g., Parrish et al., 2012, 2014).

Significant negative TOC changes (up to -2 % yr^{-1}) are also observed over the marine regions of the Atlantic Ocean, the Pacific Ocean and the Indian Ocean. The significant neg-

ative TOC changes over these regions can be associated with an increased photochemical sink (HO_x chemistry and photolysis of O_3 to (^1D)) and dilution processes due to meteorological changes (Kley et al., 1997; Wai et al., 2014). The declining trend of tropospheric O_3 over North America and Europe has also contributed to the negative TOC changes over the Oceans, mostly over the outflow regions. Changes in the amount of organic and inorganic halogens may also play a role in the observed negative TOC changes over the Oceanic regions (Dickerson et al., 1999; Read et al., 2008). Significant positive changes in tropospheric O_3 are observed over some regions of South America (region F in Fig. 7, up to $2\,\%\,yr^{-1}$), South Asia (region H in Fig. 7, 1–3 $\%\,yr^{-1}$), part of Africa (region G in Fig. 7) and over the marine regions (up to $2\,\%\,yr^{-1}$). The observed significant positive changes in tropospheric O_3 over South America, South Asia and part of Africa can be attributed to increase in population, industrialization and more energy consumption (e.g., Beig and Singh, 2007; Cooper et al., 2014). Changes in meteorology and intercontinental transport of pollution can also contribute to the observed changes in O_3 over the regions (e.g., Lelieveld et al., 2004; Beig and Singh, 2007; Parrish et al., 2012). The significant change in O_3 observed over the regions of the Southern Atlantic and southern South America can be attributed to changes in transport patterns, anthropogenic NO_x and other tropospheric O_3 precursors (e.g., Schultz et al., 1999; Wai et al., 2014). In southern Africa, the widespread biomass burning events in Angola, Zambia and the Democratic Republic of Congo, particularly during July–September lead to the formation of O_3 precursors. The transport of O_3 and its precursors by the prevailing wind systems over these regions leads to significant change in TOC (Sauvage et al., 2005, 2007a). For instance, the persistent low-level easterlies/southeasterlies in these regions facilitate the westward transport of tropospheric O_3 and its precursors (see, Fig. 2). The prevailing descending airmasses and relatively low wind speeds over southern Africa, South America, the Atlantic Ocean and the Indian Ocean limit the dispersion of tropospheric O_3 and its precursors produced from burning plumes in Africa and South America. The prevailing high-pressure system over southern Africa leads to the recirculation of plumes of tropospheric O_3 and its precursors over the continent be-

fore exiting from the southern or western part of the continent to the Indian Ocean or the Atlantic Ocean south of the ITCZ, respectively (e.g., Edwards et al., 2006; Wai et al., 2014).

Biomass burning activities in South America, which peak from August–October, lead to the formation of tropospheric O_3 and its precursors over the region. O_3 and its precursors can remain in the planetary boundary layer before they are transported to the upper troposphere via deep convective processes (e.g., Wu et al., 2011; Sauvage et al., 2006). In the free troposphere, the O_3 plumes can be effectively transported by westerlies through the continental outflows located at the southeast of South America (see, Fig. 2). The significant increase in O_3 (up to $2\,\%\,yr^{-1}$) observed over the North Australia outflow (region I) can be associated with changes in the wind pattern. The significant increase in TOC over south Asia can mainly be associated with changes in anthropogenically produced O_3 precursors from both domestic and industrial combustion as well as biomass burning (Liu et al., 2002; Parrish et al., 2012). The O_3 produced over these regions is transported towards the western Pacific Ocean by large-scale dynamics controlled by the prevailing wind systems. This can contribute to changes in O_3 over some regions of the western Pacific Ocean. The variation in TOC changes observed over the southern high latitudes may be a consequence of gaps in the TOC time series due to the applied data screening criteria described in Ebojie et al. (2014) and Ebojie (2014). This can also contribute to tropospheric O_3 variability at the Northern high latitudes.

The uncertainties of the fit parameters are determined from the covariance matrix of the regression. This is mainly a random uncertainty source, which has been analyzed using Tikhonov regularization and found not to impact the TOC trends significantly (García et al., 2012). The uncertainty in SCIAMACHY TOC has been discussed in detail by Ebojie et al. (2014) and Ebojie (2014). Additionally, the uncertainty in changes in tropospheric O_3 can arise from scanning mirror degradation and tropopause height information, but the impact of their effects on SCIAMACHY TOC is small (Bramstedt et al., 2009; Ebojie et al., 2014; Ebojie, 2014). Inspection of the the colour map of the $\%\,yr^{-1}$ and $DU\,yr^{-1}$ trend uncertainties (figures not shown) shows that the uncertainty in O_3 trend is generally below $1\,\%\,yr^{-1}$ and $0.5\,DU\,yr^{-1}$ globally, respectively (Ebojie, 2014). The uncertainties in TOC changes be-

come high at the Southern high latitudes probably due to gaps in data coverage associated with prevailing cloud cover and the variability of tropospheric ozone and its precursors in the region.

3.4.2 Regional mean tropospheric O_3 changes

Investigation of changes in the TOCs for some specific regions (Fig. 9), which are highlighted in Figs. 7 and 8, shows variability in TOCs over the years 2003–2011, which could be due to variations in meteorology and anthropogenic emissions of ozone precursors. In Table 2 and Fig. 9, five out of the eleven regions extracted from Fig. 7 show significant increase, two regions show significant decrease while the remaining four regions show insignificant change in TOCs. The changes in TOCs over these regions could be attributed to variation in tropospheric background O_3, temporal variation of precursor emissions, systematic changes in transport meteorology as well as by the changes in photochemical oxidation and removal processes. Most of the regions show a pronounced seasonal cycle with maximum TOC values during hemispheric spring and summer with different amplitudes. A significant positive change and variability in the mean tropospheric O_3 is observed over Alaska (region A). The significant positive change over this region could be a result of changes in precursors emissions from biomass burning (Stohl et al., 2007; Oltmans et al., 2010). Changes in transport from the stratosphere or lower latitudes as well as the influence of rapid climate change may also play a role (Oltmans et al., 2013). The variability in TOC over this region is high, which could probably be a result of the gaps in the TOC time series. TOC minimum is observed during 2010 winter over region B, which corresponds to Eastern North American outflow. Negative change in TOC is observed over the region, which can be associated to the declining trend in TOC over US as reported in earlier studies (Cooper et al., 2012, 2014; Parrish et al., 2012). The seasonal variation observed over regions C (Southern Europe) becomes less pronounced between 2007 and 2009. The TOC change over the region is negative, which could probably be due to reduction of O_3 precursor emissions. The region over Siberia (region D) shows significant negative change in TOC, which could probably be a result of response to emission reduc-

tion in O_3 precursor and change in anthropogenic and biogenic halogens that are effective in O_3 destruction (Parrish et al., 2012). In general, the observed significant negative change in TOC over the northern midlatitude, particularly around Europe and North America (regions B, C and D) is a combination of changes in dynamics and chemical processes. The chemical processes involve the reduction in O_3 precursor emissions and increase in anthropogenic and biogenic halogens that are effective in O_3 destruction (Vestreng et al., 2009; Parrish et al., 2012). Synoptic-scale meteorological variability and dynamical modes including changes in tropospheric circulation indices such as those of the Arctic Oscillation (AO) and the North Atlantic Oscillation NAO can play a role (Zhou et al., 2001; Chipperfield, 2003). A trend toward more equatorward planetary wave fluxes may also play a role in the negative change in tropospheric O_3 in the northern midlatitude (Kuroda and Kodera, 1999; Chen et al., 2005). Another important process that may be contributing to the decrease in tropospheric O_3 in the northern midlatitude is the decrease in the average total wave flux entering the stratosphere (Newman and Nash, 2000; Reid et al., 2000). Pronounced seasonal variation in TOC is observed over the regions of northern South America, southern South America, southern Africa, southeast Asia and North Australia outflow (Regions E–I), with each region exhibiting significant change in TOC. Strong seasonal ~~cycle~~ in TOC are also observed over Galapagos Island (region J) and the Southern Pacific Ocean (region K), with both regions showing insignificant negative change in TOC. The significant negative change in TOC observed over northern South America (region E) could be due to change in humidity and solar actinic flux (Revell et al., 2015). The significant positive change in TOC observed over regions F and G (southern South America and central Africa) is primarily due to change in pollution emission from biomass burning and anthropogenic activities (e.g., Fishman et al., 1991). The significant positive change in TOC over southeast Asia (region H) could be associated to changes in anthropogenic emissions as well as changes in transport pattern as observed by many studies (e.g., Beig and Singh, 2007; Parrish et al., 2012). Changes in population and increased industrialization in east Asia have led to great changes in anthropogenic precursor emissions over the region. The observed significant positive TOC change over northern China (i.e., part of region H) may be associated with

high O_3 over the northwestern mountainous areas during summer and in the afternoon hours (Tang et al., 2012). Over the northern Australia outflow (region I), a positive significant change in TOC is observed, which could probably be a result of changes in transport patterns and precursor emissions (Wai et al., 2014). The Galapagos Islands (region J) are among the most renowned natural sites in the world with less impact of anthropogenic activities. The observed insignificant negative change in TOC over the region could be related to synoptic-scale meteorological variability. Over the Southern Pacific Ocean (region K), insignificant negative change in TOC is observed. The insignificant negative change in TOC over the region could be associated with the influence of photochemical reactions involving hydroxyl (OH) and hydroperoxy (HO_2) radicals and change in meteorology. A summary of the changes in TOCs as well as the mean values and standard deviations over the entire time series for the different regions is shown in Table 2.

4 Summary and conclusions

In this study, changes in tropospheric O_3 columns (TOCs) were derived from SCIAMACHY limb-nadir-matching (LNM) observations during the period 2003–2011. TOC shows a statistically insignificant change in the mean O_3 of -0.2 ± 0.4, 0.3 ± 0.4, 0.1 ± 0.5 and $0.1 \pm 0.2\,\%\,yr^{-1}$ in the latitude bands 30–50° N, 20° S–0, 0–20° N and 50–30° S, respectively. From the global analysis of changes in TOC, positive changes significant at the 95 % confidence level were observed over South Asia (1–3 $\%\,yr^{-1}$), the South American continent (up to 2 $\%\,yr^{-1}$), North America, especially around Alaska (1–3 $\%\,yr^{-1}$), the Australian outflow region (up to 2 $\%\,yr^{-1}$) as well as over some regions of the African continent (up to 2 $\%\,yr^{-1}$). The positive change in O_3 over these regions could be attributed to changes in emissions of nitrogen oxides (NO_x) and other O_3 precursors. In addition, changes in meteorology and intercontinental transport of O_3 and its precursors might also have played a role in the observed changes in O_3 over the regions. Over the marine regions, significant positive TOC changes were derived over the Indian Ocean (1–2 $\%\,yr^{-1}$) and the southern Atlantic Ocean (up to 2 $\%\,yr^{-1}$). The observed positive change in TOC over the Oceanic

regions ~~could~~ be associated with changes in dynamical processes such as advection, local emissions, entrainment and transport of O_3 and its precursors from the source regions. Significant negative TOC trends were observed over some regions of Europe and the North American continent (up to $-3\,\%\,\mathrm{yr}^{-1}$), which ~~could~~ be attributed to reduction in NO_x and other tropospheric O_3 precursors emissions over the regions. Halogen chemistry might have also contributed to the observed changes in tropospheric O_3. Over the Oceanic regions including the Pacific, Atlantic and Indian Oceans, significant decrease in TOC (-1 to $-3\,\%\,\mathrm{yr}^{-1}$) was observed. The observed negative change in tropospheric O_3 over these regions ~~could~~ be associated with the influence of photochemical reactions involving hydroxyl (OH) and hydroperoxy (HO_2) radicals. Furthermore, changes in the amount of organic and inorganic halogens as well as changes in Dissolved Organic Matter (DOM) photochemistry in surface waters could be an additional source of volatile organic compounds that have contributed to the destruction of O_3. In general, changes in TOC in the observed period are smaller compared to results obtained from studies on tropospheric O_3 trends in the previous years (e.g., Marenco et al., 1994; Simmonds et al., 2004) probably due to the slowdown in the growth rate of O_3 precursors as well as changes in the lowermost stratospheric O_3 (WMO, 2011). The strengthening of legislation on air pollution related policies have contributed to the reduction of tropospheric O_3 amounts and its precursor emissions. Changes in the tropopause altitude might have also contributed to the zonal or global change in tropospheric O_3. In conclusion it can be stated that the results obtained in this paper provide first hand information on tropospheric O_3 changes both zonally and globally.

Acknowledgements. We thank ESA and German Aerospace DLR for providing SCIAMACHY level 1 data for this study. This work was funded in parts by the German Aerospace DLR project SADOS (FKZ 50EE1105), by ESA through the SCIAMACHY Quality Working Group, by Ernst-Moritz-Arndt-University of Greifswald and also by the University and State of Bremen, Germany. The SCIAMACHY instrument, which flew on ESA's Envisat spacecraft, was supported by Germany, the Netherlands and Belgium.

The article processing charges for this open-access publication were covered by the University of Bremen.

References

Appenzeller, C., Holton, J. R., and Rosenlof, K. H.: Seasonal variation of mass transport across the tropopause, J. Geophys. Res., 101, 15071–15078, doi:10.1029/96JD00821, 1996.

Baldwin, M. P., Gray, L. J., Dunkerton, T. J., Hamilton, K., Haynes, P. H., Randel, W. J., Holton, J. R., Alexander, M. J., Hirota, I., Horinouchi, T., Jones, D. B. A., Kinnersley, J. S., Marquardt, C., Sato, K., and Takahashi, M.: The quasi-biennial oscillation, Rev. Geophys., 39, 179–230, doi:10.1029/1999RG000073, 2001.

Beig, G. and Singh, V.: Trends in tropical tropospheric column ozone from satellite data and MOZART model, Geophys. Res. Lett., 34, L17801, doi:10.1029/2007GL030460, 2007.

Bjerknes, J.: A possible response of the atmospheric hadley circulation to equatorial anomalies of ocean temperature, Tellus, 18, 820–829, 1966.

Bramstedt, K., Noël, S., Bovensmann, H., Burrows, J. P., Lerot, C., Tilstra, L. G., Lichtenberg, G., Dehn, A., and Fehr, T.: SCIAMACHY Monitoring Factors: Observation and End-to-End Correction of Instrument Performance Degradation, in: Atmospheric Science Conference, SP-676, 7–11, Barcelona, Spain, September 2009.

Brasseur, G. P., Orlando, J. J., and Tyndall, G. S.: Atmospheric Chemistry and Global Change, Oxford Univ. Press, New York, 1999.

Butchart, N., Scaife, A. A., Austin, J., Hare, S. H. E., and Knight, J. R.: Quasi-biennial oscillation in ozone in a coupled chemistry-climate model, J. Geophys. Res., 108, 2156–2202, doi:10.1029/2002JD003004, 2003.

Chandra, S., Ziemke, J. R., Min, W., and Read, W. G.: Effects of 1997–1998 El Nino on tropospheric ozone and water vapor, Geophys. Res. Lett., 25, 3867–3870, 1998.

Chandra, S., Ziemke, J. R., Bhartia, P. K., and Martin, R. V.: Tropical tropospheric ozone: implications for dynamics and biomass burning, J. Geophys. Res., 107, 4188, doi:10.1029/2001JD000447, 2002.

Chandra, S., Ziemke, J. R., and Martin, R. V.: Tropospheric ozone at tropical and middle latitudes derived from TOMS/MLS residual: comparison with a global model, J. Geophys. Res., 108, 4291, doi:10.1029/2002JD002912, 2003.

Chandra, S., Ziemke, J. R., Tie, X., and Brasseur, G.: Elevated ozone in the troposphere over the Atlantic and Pacific oceans in the Northern Hemisphere, Geophys. Res. Lett., 31, L23102, doi:10.1029/2004GL020821, 2004.

Chen, W., Yang, S., and Huang, R. H.: Relationship between stationary planetary wave activity and the East Asian winter monsoon, J. Geophys. Res., 110, D14110, doi:10.1029/2004JD005669, 2005.

Chipperfield, M. P.: A three-dimensional model study of long-term mid-high latitude lower stratosphere ozone changes, Atmos. Chem. Phys., 3, 1253–1265, doi:10.5194/acp-3-1253-2003, 2003.

Coldewey-Egbers, M., Loyola R., D. G., Braesicke, P., Dameris, M., van Roozendael, M., Lerot, C., and Zimmer, W.: A new health check of the ozone layer at global and regional scales, Geophys. Res. Lett., 41, 1–10, doi:10.1002/2014GL060212, 2014.

Cooper, O. R. and Parrish, D. D.: Air pollution export from and import to North America, in: Inter-Continental Transport of Air Pollution, edited by: Stohl, A., Springer, New York, 41–67, 4G, doi:10.1007/b94523, 2004.

Cooper, O. R., Gao, R. S., Tarasick, D., Leblanc, T., and Sweeney, J.: Long-term ozone trends at rural ozone monitoring sites across the United States, 1990–2010, J. Geophys. Res., 117, D22307, doi:10.1029/2012JD018261, 2012.

Cooper, O. R., Parrish, D. D., Ziemke, J., Balashov, N. V., Cupeiro, M., Galbally, I. E., Gilge, S., Horowitz, L., Jensen, N. R., Lamarque, J.-F., Naik, V., Oltmans, S. J., Schwab, J., Shindell, D. T., Thompson, A. M., Thouret, V., Wang, Y., and Zbinden, R. M.: Global distribution and trends of tropospheric ozone: an observation-based review, Elementa: Science of the Anthropocene, 2, 000029, doi:10.12952/journal.elementa.000029, 2014.

Crutzen, P. J.: The role of NO and NO_2 in the chemistry of the troposphere and stratosphere, Annu. Rev. Earth Pl. Sc., 7, 443–472, 1979.

Danielsen, E. F.: Stratospheric-tropospheric exchange based on radioactivity, ozone and potential vorticity, J. Atmos. Sci., 25, 502–518, 1968.

de Laat, A. T. J., Aben, I., and Roelofs, G. J.: A model perspective on total tropospheric O_3 column variability and implications for satellite observations, J. Geophys. Res., 110, D13303, doi:10.1029/2004JD005264, 2005.

Dentener, F., Stevenson, D., Cofala, J., Mechler, R., Amann, M., Bergamaschi, P., Raes, F., and Derwent, R.: The impact of air pollutant and methane emission controls on tropospheric ozone and radiative forcing: CTM calculations for the period 1990–2030, Atmos. Chem. Phys., 5, 1731–1755, doi:10.5194/acp-5-1731-2005, 2005.

Derwent, R., Simmonds, P., Seuring, S., and Dimmer, C.: Observation and interpretation of the seasonal cycles in the surface concentrations of ozone and carbon monoxide at Mace Head, Ireland from 1990 to 1994, Atmos. Environ., 32, 145–157, 1998.

Derwent, R. G., Jenkin, M. E., Saunders, S. M., Pilling, M. J., Simmonds, P. G., Passant, N. R., Dollard, G. J., Dumitrean, P., and Kent, A.: A photochemical ozone formation in north west Europe and its control, Atmos. Environ., 37, 1983–1991, 2003.

Dickerson, R. R., Doddridge, B. G., Kelley, P. K., and Rhoads, K. P.: Large-scale pollution of the atmosphere over the North Atlantic Ocean: evidence from Bermuda, J. Geophys. Res., 100, 8945–8952, 1995.

Dickerson, R. R., Rhoads, K. P., Carsey, T. P., Oltmans, S. J., Burrows, J. P., and Crutzen, P. J.: Ozone in the remote marine boundary layer: a possible role for halogens, J. Geophys. Res., 104, 21385–21395, 1999.

Doughty, D. C., Thompson, A. M., Schoeberl, M. R., Stajner, I., Wargan, K., and Hui, W. C. J.: An intercomparison of tropospheric ozone retrievals derived from two Aura instruments and measurements in western North America in 2006, J. Geophys. Res., 116, D06303, doi:10.1029/2010JD014703, 2011.

Duncan, B. N., Yoshida, Y., Olson, J. R., Sillman, S., Martin, R. V., Lamsal, L., Hu, Y., Pickering, K. E., Retscher, C., Allen, D. J., and Crawford, J. H.: Application of OMI observations to a space-based indicator of NO_x and VOC controls on surface ozone formation, Atmos. Environ., 44, 2213–2223, 2010.

Ebojie, F., von Savigny, C., Ladstätter-Weißenmayer, A., Rozanov, A., Weber, M., Eichmann, K.-U., Bötel, S., Rahpoe, N., Bovensmann, H., and Burrows, J. P.: Tropospheric column amount of ozone retrieved from SCIAMACHY limb–nadir-matching observations, Atmos. Meas. Tech., 7, 2073–2096, doi:10.5194/amt-7-2073-2014, 2014.

Ebojie, F.: Tropospheric ozone columns retrieval from SCIAMACHY limb-nadir-matching observations (Ph.D. dissertation), Universität Bremen: Physik/Elektrotechnik, , 213, 2014.

Eckert, E., von Clarmann, T., Kiefer, M., Stiller, G. P., Lossow, S., Glatthor, N., Degenstein, D. A., Froidevaux, L., Godin-Beekmann, S., Leblanc, T., McDermid, S., Pastel, M., Steinbrecht, W., Swart, D. P. J., Walker, K. A., and Bernath, P. F.: Drift-corrected trends and periodic variations in MIPAS IMK/IAA ozone measurements, Atmos. Chem. Phys., 14, 2571–2589, doi:10.5194/acp-14-2571-2014, 2014.

Edwards, D. P., Emmons, L. K., Gille, J. C., Chu, A., Attié, J.-L., Giglio, L., Wood, S. W., Haywood, J., Deeter, M. N., Massie, S. T., Ziskin, D. C., and Drummond, J. R.: Satellite observed pollution from Southern Hemisphere biomass burning, J. Geophys. Res., 111, D14312, doi:10.1029/2005JD006655, 2006.

Finlayson-Pitts, B. J., Livingston, F. E., and Pitts Jr., J. N.: Ozone destruction and bromine photochemistry at ground level in the Arctic spring, Nature, 343, 622–625, doi:10.1038/343622a0, 1990.

Fiore, A. M., Dentener, F. J., Wild, O., Cuvelier, C., Schultz, M. G., Hess, P., Textor, C., Schulz, M., Doherty, R. M., Horowitz, L. W., MacKenzie, I. A., Sanderson, M. G., Shindell, D. T., Stevenson, D. S., Szopa, S., Van Dingenen, R., Zeng, G., Atherton, C., Bergmann, D., Bey, I., Carmichael, G., Collins, W. J., Duncan, B. N., Faluvegi, G., Folberth, G., Gauss, M., Gong, S., Hauglustaine, D., Holloway, T., Isaksen, I. S. A., Jacob, D. J., Jonson, J. E., Kaminski, J. W., Keating, T. J., Lupu, A., Marmer, E., Montanaro, V., Park, R. J., Pitari, G., Pringle, K. J., Pyle, J. A., Schroeder, S., Vivanco, M. G., Wind, P., Wojcik, G., Wu, S., and Zuber, A.: Multimodel estimates of intercontinental source–receptor relationships for ozone pollution, J. Geophys. Res., 114, D04301, doi:10.1029/2008JD010816, 2009.

Fishman, J., Watson, C., Larsen, J., and Logan, J.: Distribution of tropospheric ozone determined from satellite data, J. Geophys. Res., 95, 3599–3617, 1990.

Fishman, J., Fakhruzzaman, K., Cros, B., and Nganda, D.: Identification of widespread pollution in the Southern Hemisphere deduced from satellite analyses, Science, 252, 5013, 1693–1696, doi:10.1126/science.252.5013.1693, 1991.

Fujiwara, M., Kita, K., Kawakami, S., Ogawa, T., Komala, N., Saraspriya, S., and Suripto, A.: Tropospheric ozone enhancements during the Indonesian forest fire events in 1994 and in 1997 as revealed by ground-based observations, Geophys. Res. Lett., 26, 2417–2420, 1999.

Fusco, A. C. and Logan, J. A.: Analysis of 1970–1995 trends in tropospheric ozone at Northern Hemisphere midlatitudes with the GEOS-CHEM model, J. Geophys. Res., 108, 4449, doi:10.1029/2002JD002742, 2003.

García, O. E., Schneider, M., Redondas, A., González, Y., Hase, F., Blumenstock, T., and Sepúlveda, E.: Investigating the long-term evolution of subtropical ozone profiles applying ground-based FTIR spectrometry, Atmos. Meas. Tech., 5, 2917–2931, doi:10.5194/amt-5-2917-2012, 2012.

Garfinkel, C. I. and Hartmann, D. L.: The influence of the quasi-biennial oscillation on the troposphere in winter in a hierarchy of models, Part I: simplified dry GCMS, J. Atmos. Sci., 68, 1273–1289, doi:10.1175/2011JAS3665.1, 2011.

Gebhardt, C., Rozanov, A., Hommel, R., Weber, M., Bovensmann, H., Burrows, J. P., Degenstein, D., Froidevaux, L., and Thompson, A. M.: Stratospheric ozone trends and variability as seen by SCIA-

MACHY from 2002 to 2012, Atmos. Chem. Phys., 14, 831–846, doi:10.5194/acp-14-831-2014, 2014.
Gentner, D. R., Ormeño, E., Fares, S., Ford, T. B., Weber, R., Park, J.-H., Brioude, J., Angevine, W. M., Karlik, J. F., and Goldstein, A. H.: Emissions of terpenoids, benzenoids, and other biogenic gas-phase organic compounds from agricultural crops and their potential implications for air quality, Atmos. Chem. Phys., 14, 5393–5413, doi:10.5194/acp-14-5393-2014, 2014.
Guenther, A., Geron, C., Pierce, T., Lamb, B., Harley, P., and Fall, R.: Natural emissions of non-methane volatile organic compounds; carbon monoxide, and oxides of nitrogen from North America, Atmos. Environ., 34, 2205–2230, 2000.
Haigh, J. D., Blackburn, M., and Day, R.: The response of tropospheric circulation to perturbations in lower-stratospheric temperature, J. Climate, 18, 3672–3685, doi:10.1175/JCLI3472.1, 2005.
Hao, J. and Wang, L.: Chemistry and physiology of Los Angeles smog, Ind. Eng. Chem., 44, 1342–1346, 1952.
Holton, J. R. and Tan, H. C.: The influence of the equatorial QBO in the global circulation at 50 mb, J. Atmos. Sci., 37, 2200–2208, 1980.
Hudson, R. D.: Measurements of the movement of the jet streams at mid-latitudes, in the Northern and Southern Hemispheres, 1979 to 2010, Atmos. Chem. Phys., 12, 7797–7808, doi:10.5194/acp-12-7797-2012, 2012.
Jacob, D. J. and Winner, D. A.: Effect of climate change on air quality, Atmos. Environ., 43, 51–63, doi:10.1016/j.atmosenv.2008.09.051, 2009.
Jacob, D. J., Logan, J. A., and Murti, P. P.: Effect of rising Asian emissions on surface ozone in the United States, Geophys. Res. Lett., 26, 2175–2178, 1999.
Jacobson, M. Z.: Air Pollution and Global Warming: History, Science, and Solutions, 2nd edn., Cambridge Univ. Press, Cambridge, 2012.
Jaffe, D. A., Anderson, T., Covert, D., Kotchenruther, R., Trost, B., Danielson, J., Simpson, W., Bertsen, T., Karlsdottir, S., Blake, D., Harris, J., Carmichael, G., and Uno, I.: Transport of Asian air pollution to North America, Geophys. Res. Lett., 26, 711–714, 1999.
Kim, J. H. and Newchurch, M. J.: Climatology and trends of tropospheric ozone over the eastern Pacific Ocean: The influences of biomass burning and tropospheric dynamics, Geophys. Res. Lett., 23, 3723–3726, doi:10.1029/96GL03615, 1996.
Kley, D., Smit, H. G. J., Vómel, H., Grassl, H., Ramanathan, V., Crutzen, P. J., Williams, S., J., M., and Oltmans, S.: Tropospheric water vapour and ozone cross-sections in a zonal plane over the central equatorial Pacific, Q. J. Roy. Meteor. Soc., 123, 2009–2040, 1997.

Kuroda, Y. and Kodera, K.: Role of planetary waves in the stratosphere-troposphere coupled variability in the Northern Hemisphere winter, Geophys. Res. Lett., 26, 2375–2378, 1999.

Ladstädter-Weissenmayer, A., Burrows, J. P., Crutzen, P. J., and Richter, A.: GOME: Biomass burning and its influence on the troposphere, in: European Symposium on Atmospheric Measurements from Space, ESA WPP-161, ESA/ESTEC, Noordwijk, The Netherlands, 369–374, 1999.

Lamarque, J. F. and Hess, P. G.: Cross-tropopause mass exchange and potential vorticity budget in a simulated tropopause folding., J. Atmos. Sci., 51, 2246–2269, 1994.

Lee, S., Shelow, D. M., Thompson, A. M., and Miller, S. K.: QBO and ENSO variability in temperature and ozone from SHADOZ, 1998–2005, J. Geophys. Res., 115, D18105, doi:10.1029/2009JD013320, 2010.

Lelieveld, J. and Dentener, F. J.: What controls tropospheric ozone?, J. Geophys. Res., 105, 3531–3551, doi:10.1029/1999JD901011, 2000.

Lelieveld, J., van Aardenne, J., Fischer, H., de Reus, M., Williams, J., and Winkler, P.: Increasing ozone over the Atlantic Ocean, Science, 304, 1483–1487, 2004.

Levy, H. I.: Normal atmosphere: large radical and formaldehyde concentrations predicted, Science, 173, 141–143, 1971.

Lippmann, M.: Health-effects of tropospheric ozone, Environ. Sci. Technol., 25, 1954–1962, 1991.

Liu, H., Jacob, D. J., Chan, L. Y., Oltmans, S. J., Bey, I., Yantosca, R. M., Harris, J. M., Duncan, B. N., and Martin, R. V.: Sources of tropospheric ozone along the Asian Pacific Rim: an analysis of ozonesonde observations, J. Geophys. Res., 107, 4573, doi:10.1029/2001JD002005, 2002.

Logan, J. A., Prather, M. J., Wofsy, S. C., and McElroy, M. B.: Tropospheric chemistry: a global perspective, J. Geophys. Res., 86, 7210–7255, 1981.

Logan, J. A., Staehelin, J., Megretskaia, I. A., Cammas, J.-P., Thouret, V., Claude, H., De Backer, H., Steinbacher, M., Scheel, H.-E., Stübi, R., Fröhlich, M., and Derwent, R.: Changes in ozone over Europe: analysis of ozone measurements from sondes, regular aircraft (MOZAIC) and alpine surface sites, J. Geophys. Res., 117, D09301, doi:10.1029/2011JD016952, 2012.

Marenco, A., Gouget, H., Nédélec, P., Pagés, J. P., and Karcher, F.: Evidence of a long-term increase in tropospheric ozone from Pic du Midi data series: consequences: positive radiative forcing, J. Geophys. Res., 99, 16617–16632, 1994.

Milford, J. B., Russell, A. G., and McRae, G. J.: A new approach to photochemical pollution control: implications of spatial patterns in pollutant responses to reductions in nitrogen oxides and reactive organic gas emissions, Environ. Sci. Technol., 23, 1290–1301, 1989.

Monks, P. S.: Gas-phase radical chemistry in the troposphere, Chem. Soc. Rev., 34, 376–395, doi:10.1039/B307982C, 2005.

Moxim, W. J. and Levy II, H.: A model analysis of the tropical South Atlantic Ocean tropospheric ozone maximum: The interaction of transport and chemistry, J. Geophys. Res., 105, 17393–17415, 2000.

Naja, M., Akimoto, H., and Staehelin, J.: Ozone in background and photochemically aged air over central Europe: Analysis of long-term ozonesonde data from Hohenpeissenberg and Payerne, J. Geophys. Res., 108, 4063, doi:10.1029/2002JD002477, 2003.

Neu, J. L., Flury, T., Manney, G. L., Santee, M. L., Livesey, N. J., and Worden, J.: Tropospheric ozone variations governed by changes in stratospheric circulation, Nat. Geosci., 340–344, 7, doi:10.1038/ngeo2138, 2014.

Newman, P. A. and Nash, E. R.: Quantifying the wave driving of the stratosphere, J. Geophys. Res., 105, 12485–12497, 2000.

Oltmans, S. J., Lefohn, A. S., Shadwick, D., Harris, J. M., Scheel, H. E., Galbally, I., Tarasick, D. W., Johnson, B. J., Brunke, E. G., Claude, H., Zeng, G., Nichol, S., Schmidlin, F., Davies, J., Cuevas, E., Redondas, A., Naoe, H., Nakano, T., Kawasato, T.: Recent tropospheric ozone changes – A pattern dominated by slow or no growth, Atmos. Environ., 67, 331–351, doi:10.1016/j.atmosenv.2012.10.057, 2013.

Oltmans, S. J., Lefohn, A. S., Harris, J. M., Tarasick, D. W., Thompson, A. M., Wernli, H., Johnson, B. J., Davies, J., Novelli, P., Montzka, S., Sweeney, C., Patrick, L. C., Jefferson, A., Dann, T., Ray, J. D., Shapiro, M., Holben, B. N.: Enhanced ozone over western North America from biomass burning in Eurasia during April 2008 as seen in surface and profile observations, Atmos. Environ., 44, 4497–4509, 10.1016/j.atmosenv.2010.07.004, 2010.

Oltmans, S. J., Lefohn, A. S., Harris, J. M., Galbally, I., Scheel, H. E., Bodeker, G., Brunke, E., Claude, H., Tarasick, D. W., Johnson, B. J., Simmonds, P., Shadwick, D., Anlauf, K., Hayden, K., Schmidlin, F., Fujimoto, T., Akagi, K., Meyer, C., Nichol, S., Davies, J., Redondas, A., and Cuevas, E.: Long-term changes in tropospheric ozone, Atmos. Environ., 40, 3156–3173, doi:10.1029/2008JD010378, 2006.

Oman, L. D., Douglass, A. R., Ziemke, J. R., Rodriguez, J. M., Waugh, D. W., and Nielsen, J. E.: The ozone response to ENSO in Aura satellite measurements and a chemistry–climate simulation, J. Geophys. Res.-Atmos., 118, 965–976, 2013.

Parrish, D. D., Holloway, J. S., Trainer, M., Murphy, P. C., Forbes, G. L., and Fehsenfeld, F. C.: Export of North American ozone pollution to the North Atlantic Ocean, Science, 259, 1436–1439, 1993.

Parrish, D. D., Law, K. S., Staehelin, J., Derwent, R., Cooper, O. R., Tanimoto, H., Volz-Thomas, A., Gilge, S., Scheel, H.-E., Steinbacher, M., and Chan, E.: Long-term changes in lower tropospheric baseline ozone concentrations at northern mid-latitudes, Atmos. Chem. Phys., 12, 11485–11504, doi:10.5194/acp-12-11485-2012, 2012.

Parrish, D. D., Law, K. S., Staehelin, J., Derwent, R., Cooper, O. R., Tanimoto, H., Volz-Thomas, A., Gilge, S., Scheel, H. E., Steinbacher, M., and Chan, E.: Lower tropospheric ozone at northern mid-latitudes: changing seasonal cycle, Geophys. Res. Lett., 40, 1631–1636, doi:10.1002/grl.50303, 2013.

Parrish, D. D., Lamarque, J.-F., Naik, V., Horowitz, L., Shindell, D. T., Staehelin, J., Derwent, R., Cooper, O. R., Tanimoto, H., Volz-Thomas, A., Gilge, S., Scheel, H.-E., Steinbacher, M., and Fröhlich, M.: Long-term changes in lower tropospheric baseline ozone concentrations: comparing chemistry-climate models and observations at northern midlatitudes, J. Geophys. Res.-Atmos., 119, 5719–5736, doi:10.1002/2013JD021435, 2014.

Pascoe, C. L., Gray, L. J., Crooks, S. A., Juckes, M. N., and Baldwin, M. P.: The quasi-biennial oscillation: analysis using ERA-40 data, J. Geophys. Res., 110, D08105, doi:10.1029/2004JD004941, 1948.

Pfister, G. G., Emmons, L. K., Hess, P. G., Lamarque, J.-F., Thompson, A. M., and Yorks, J. E.: Analysis of the Summer 2004 ozone budget over the United States using Intercontinental Transport Experiment Ozonesonde Network Study (IONS) observations and Model of Ozone and Related Tracers (MOZART-4) simulations, J. Geophys. Res., 113, D23306, doi:10.1029/2008JD010190, 2008.

Randel, W. and Thompson, A.: Interannual variability and trends in tropical ozone derived from SAGE II satellite data and SHADOZ ozonesondes, J. Geophys. Res., 116, D07303, doi:10.1029/2010JD015195, 2011.

Read, K. A., Mahajan, A. S., Carpenter, L. J., Evans, M. J., Faria, B. V. E., Heard, D. E., Hopkins, J. R., Lee, J. D., Moller, S. J., Lewis, A. C., Mendes, L., McQuaid, J. B., Oetjen, H., Saiz-Lopez, A., Pilling, M. J., and Plane, J. M. C.: Extensive halogen-mediated ozone destruction over the tropical Atlantic Ocean, Nature, 453, 1232–1235, 2008.

Reid, S. J., Tuck, A. F., and Kildaris, G.: On the changing abundance of ozone minima at Northern midlatitudes, J. Geophys. Res., 105, 12169–12180, 2000.

Revell, L. E., Tummon, F., Stenke, A., Sukhodolov, T., Coulon, A., Rozanov, E., Garny, H., Grewe, V., and Peter, T.: Drivers of the tropospheric ozone budget throughout the 21st century under the

medium-high climate scenario RCP 6.0, Atmos. Chem. Phys., 15, 5887–5902, doi:10.5194/acp-15-5887-2015, 2015.

Romanski, J., Romanou, A. Bauer, M. and Tselioudis, G.: Teleconnections, midlatitude cyclones and Aegean Sea turbulent heat flux variability on daily through decadal time scales. Reg. Environ. Change, 14, 5, 1713–1723, doi:,10.1007/s10113-013-0545-0,2014.

Santer, B. D., Sausen, R., Wigley, T. M. L., Boyle, J. S., AchutaRao, K., Doutriaux, C., Hansen, J. E., Meehl, G. A., Roeckner, E., Ruedy, R., Schmidt, G., and Taylor, K. E.: Behavior of tropopause height and atmospheric temperature in models, reanalyses, and observations: decadal changes, J. Geophys. Res., 108, 4002, 2003a.

Santer, B. D., Wehner, M. F., Wigley, T. M. L., Sausen, R., Meehl, G. A., Taylor, K. E., Ammann, C., Arblaster, J., Washington, W. M., Boyle, J. S., and Brüggemann, W.: Contributions of anthropogenic and natural forcing to recent tropopause height changes, Science, 301, 479–483, 2003b.

Sauvage, B., Thouret, V., Cammas, J.-P., Gheusi, F., Athier, G., and Nédélec, P.: Tropospheric ozone over Equatorial Africa: regional aspects from the MOZAIC data, Atmos. Chem. Phys., 5, 311–335, doi:10.5194/acp-5-311-2005, 2005.

Sauvage, B., Thouret, V., Thompson, A. M., Witte, J. C., Cammas, J. P., Nédélec, P., and Athier, G.: Enhanced view of the tropical Atlantic ozone paradox and zonal wave one from the in situ MOZAIC and SHADOZ data, J. Geophys. Res., 111, D01301, doi:10.1029/2005JD006241, 2006.

Sauvage, B., Gheusi, F., Thouret, V., Cammas, J.-P., Duron, J., Escobar, J., Mari, C., Mascart, P., and Pont, V.: Medium-range mid-tropospheric transport of ozone and precursors over Africa: two numerical case studies in dry and wet seasons, Atmos. Chem. Phys., 7, 5357–5370, doi:10.5194/acp-7-5357-2007, 2007a.

Sauvage, B., Martin, R. V., van Donkelaar, A., and Ziemke, J. R.: Quantification of the factors controlling tropical tropospheric ozone and the South Atlantic maximum, J. Geophys. Res., 112, D11309, doi:10.1029/2006JD008008, 2007b.

Schultz, M. G., Jacob, D. J., Wang, Y., Logan, J. A., Atlas, E. L., Blake, D. R., Blake, N. J., Bradshaw, J. D., Browell, E. V., Fenn, M. A., Flocke, F., Gregory, G. L., Heikes, B. G., Sachse, G. W., Sandholm, S. T., Shetter, R. E., Singh, H. B., and Talbot, R. W.: On the origin of tropospheric ozone and NO_x over the tropical South Pacific, J. Geophys. Res., 104, 5829–5843, doi:10.1029/98JD02309, 1999.

Shindell, D. T., Faluvegi, G., Lacis, A., Hansen, J., Ruedy, R., and Aguilar, E.: Role of tropospheric ozone increases in 20th-century climate change, J. Geophys. Res., 111, D08302, doi:10.1029/2005JD006348, 2006.

Sillman, S., Logan, J. A., and Wofsy, S. C.: The sensitivity of ozone to nitrogen oxides and hydrocarbons in regional ozone episodes, J. Geophys. Res., 95, 1837–1851, doi:10.1029/JD095iD02p01837, 1990.

Simmonds, P. G., Derwent, R. G., Manning, A. L., and Spain, G.: Significant growth in surface ozone at Mace Head, Ireland, 1987–2003, Atmos. Environ., 38, 4769–4778, 2004.

Simpson, I. R., Shepherd, T. G., and Sigmond, M.: Dynamics of the lower stratospheric circulation response to ENSO, J. Atmos. Sci., 68, 2537–2556, 2011.

Stiller, G. P., von Clarmann, T., Haenel, F., Funke, B., Glatthor, N., Grabowski, U., Kellmann, S., Kiefer, M., Linden, A., Lossow, S., and López-Puertas, M.: Observed temporal evolution of global mean age of stratospheric air for the 2002 to 2010 period, Atmos. Chem. Phys., 12, 3311–3331, doi:10.5194/acp-12-3311-2012, 2012.

Stohl, A., Forster, C., Huntrieser, H., Mannstein, H., McMillan, W. W., Petzold, A., Schlager, H., and Weinzierl, B.: Aircraft measurements over Europe of an air pollution plume from Southeast Asia – aerosol and chemical characterization, Atmos. Chem. Phys., 7, 913–937, doi:10.5194/acp-7-913-2007, 2007.

Tang, G., Wang, Y., Li, X., Ji, D., Hsu, S., and Gao, X.: Spatial-temporal variations in surface ozone in Northern China as observed during 2009–2010 and possible implications for future air quality control strategies, Atmos. Chem. Phys., 12, 2757–2776, doi:10.5194/acp-12-2757-2012, 2012.

Thompson, A. M., Doddridge, B. G., Witte, J. C., Hudson, R. D., Luke, W. T., Johnson, J. E., Johnson, B. J., Oltmans, S. J., and Weller, R.: A tropical Atlantic paradox: shipboard and satellite views of a tropospheric ozone maximum and wave-one in January–February 1999, Geophys. Res. Lett., 27, 3317–3320, 2000.

Thompson, A. M., Witte, J. C., Hudson, R. D., Guo, H., Herman, J. R., and Fujiwara, M.: Tropical tropospheric ozone and biomass burning, Science, 291, 2128–2132, 2001.

Thompson, A. M., Yorks, J. E., Miller, S. K., Witte, J. C., Dougherty, K. M., Morris, G. A., Baumgardner, D., Ladino, L., and Rappenglück, B.: Tropospheric ozone sources and wave activity over Mexico City and Houston during MILAGRO/Intercontinental Transport Experiment (INTEX-B) Ozonesonde Network Study, 2006 (IONS-06), Atmos. Chem. Phys., 8, 5113–5125, doi:10.5194/acp-8-5113-2008, 2008.

Thompson, A. M., Balashov, N. V., Witte, J. C., Coetzee, J. G. R., Thouret, V., and Posny, F.: Tropospheric ozone increases over the southern Africa region: bellwether for rapid growth in Southern Hemisphere pollution?, Atmos. Chem. Phys., 14, 9855–9869, doi:10.5194/acp-14-9855-2014, 2014.

Tiao, G. C., Reinsel, G. C., Xu, D., Pedrick, J. H., Zhu, X., Miller, A. J., DeLuisi, J. J., Mateer, C. L., and Wuebbles, D. J.: Effects of autocorrelation and temporal sampling schemes on estimates of trend and spatial correlation, J. Geophys. Res., 95, 20507–20517, 1990.

TOR-2: Tropspheric Ozone Research, Eurotrac-2 Subproject Final Report, ISS GSF-National Research Center for Environment and Health, Munich, Germany, 2003.

Trenberth, K. E., Stepaniak, D. P., and Caron, J. M.: The global monsoon as seen through the divergent atmospheric circulation, J. Climate, 13, 3969–3993, 2000.

Valks, P., Hao, N., Gimeno Garcia, S., Loyola, D., Dameris, M., Jöckel, P., and Delcloo, A.: Tropical tropospheric ozone column retrieval for GOME-2, Atmos. Meas. Tech., 7, 2513–2530, doi:10.5194/amt-7-2513-2014, 2014.

Vestreng, V., Ntziachristos, L., Semb, A., Reis, S., Isaksen, I. S. A., and Tarrasón, L.: Evolution of NO_x emissions in Europe with focus on road transport control measures, Atmos. Chem. Phys., 9, 1503–1520, doi:10.5194/acp-9-1503-2009, 2009.

von Clarmann, T., Stiller, G., Grabowski, U., Eckert, E., and Orphal, J.: Technical Note: Trend estimation from irregularly sampled, correlated data, Atmos. Chem. Phys., 10, 6737–6747, doi:10.5194/acp-10-6737-2010, 2010.

von Glasow, R., Sander, R., Bott, A., and Crutzen, P. J.: Modelling halogen chemistry in the marine boundary layer, 1. Cloud-free MBL, J. Geophys. Res., 107, 4341–4356, 2002.

Wai, K. M., Wu, S., Kumar, A., and Liao, H.: Seasonal variability and long-term evolution of tropospheric composition in the tropics and Southern Hemisphere, Atmos. Chem. Phys., 14, 4859–4874, doi:10.5194/acp-14-4859-2014, 2014.

Wang, C. ENSO, Atlantic climate variability, and the Walker and Hadley circulations. In: The Hadley Circulation: Present, Past, and Future. H.F. Diaz and R.S. Bradley, Eds., Kluwer Academic Publishers, 173–202, 2005.

Weatherhead, E. C., Reinsel, G. C., Tiao, G. C., Jackman, C. H., Bishop, L., Frith, S. M. H., DeLuisi, J., Keller, T., Oltmans, S. J.,Fleming, E. L., Wuebbles, D. J., Kerr, J. B., Miller, A. J., Herman, J., McPeters, R., Nagatani, R. M., and Frederick, J. E.: Detecting the recovery of total column ozone, J. Geophys. Res., 105, 22201–22210, doi:10.1029/2000JD900063, 2000.

Wild, O. and Akimoto, H.: Intercontinental transport of ozone and its precursors in a three-dimensional global CTM, J. Geophys. Res., 106, 27729–27744, doi:10.1029/2000JD000123, 2001.

WMO: World Meteorological Organization, Scientific Assessment of Ozone Depletion: 1998, Global Ozone Research and Monitoring Project–Report No. 44, Geneva, WMO 44, Geneva, Switzerland, 1999.

WMO (World Meteorological Organization), Scientific Assessment of Ozone Depletion: 2010, Global Ozone Research and Monitoring Project-Report No. 52, 516 p., Geneva, Switzerland, 2011.

Wu, L., Su, H., and Jiang, J. H.: Regional simulations of deep convection and biomass burning over South America: 1. Model evaluations using multiple satellite data sets, J. Geophys. Res., 116, D17208, doi:10.1029/2011JD016105, 2011.

Ye, D. Z. and Wu, G.: The role of the heat source of the Tibetan Plateau in the general circulations, Meteorol. Atmos. Phys., 67, 181–198, doi:10.1007/BF01277509, 1998.

Zeng, G. and Pyle, J. A.: Influence of El Niño Southern Oscillation on stratosphere/troposphere exchange and the global ozone budget, Geophys. Res. Lett., 32, L01814, doi:10.1029/2004GL021353, 2005.

Zhang, J., Rao, S. T., and Daggupaty, S. M.: Meteorological processes and ozone exceedances in the northeastern United States during the 12–16 July 1995 episode, J. Appl. Meteorol., 37, 776–789, 1998.

Zhang, P., Yang, S., and Kousky, W. E.: South Asian High and Asian-Pacific-American climate teleconnection, Adv. Atmos. Sci., 22, 915–923, doi:10.1007/BF02918690, 2005.

Zhou, S., Miller, A. J., Wang, J., and Angell, J.: Trends of NAO and AO and their associations with stratospheric processes, Geophys. Res. Lett., 28, 4107–4110, 2001.

Ziemke, J. R., Chandra, S., and Bhartia, P. K.: A 25-year data record of atmospheric ozone in the Pacific from Total Ozone Mapping Spectrometer (TOMS) cloud slicing: implications for ozone trends in the stratosphere and troposphere, J. Geophys. Res., 110, D15105, doi:10.1029/2004JD005687, 2005.

Ziemke, J. R., Olsen, M. A., Witte, J. C., Douglass, A. R., Strahan, S. E., Wargan, K., Liu, X., Schoeberl, M. R., Yang, K., Kaplan, T. B., Pawson, S., Duncan, B. N., Newman, P. A., Bhartia, P. K., and Heney, M. K.: Assessment and applications of NASA ozone data products derived from Aura OMI/MLS satellite measurements in context of the GMI chemical transport model, J. Geophys. Res.-Atmos., 119, 5671–5699, doi:10.1002/2013JD020914, 2014.

Table 1. Trend analysis results for SCIAMACHY tropospheric O_3 for different latitude ranges. Also included are mean values and standard deviation over the entire time series.

Lat. range	Mean value and SD (DU)	Trend (% yr^{-1})
70–50° S	24.8 ± 3.7	0.0 ± 0.3
50–30° S	30.4 ± 4.9	0.1 ± 0.2
30–10° S	31.1 ± 4.7	0.3 ± 0.3
10° S–10° N	26.1 ± 3.1	0.1 ± 0.5
20° S–0	27.5 ± 3.9	0.3 ± 0.4
0–20° N	29.3 ± 2.7	0.1 ± 0.5
10–30° N	33.9 ± 2.6	0.2 ± 0.5
30–50° N	39.0 ± 3.9	-0.2 ± 0.4
50–70° N	35.9 ± 6.3	-0.4 ± 0.4

Table 2. Trend analysis results for SCIAMACHY tropospheric O_3 for different regions. Also included are mean values and standard deviation over the entire time series. Bold text indicates statistically significant changes in TOC.

Region	Lat. range	Long. range	Mean value and SD (DU)	Trend (% yr^{-1})
A. Alaska	**60–70° N**	**165–130° W**	36.7 ± 11.0	1.4 ± 0.6
B. North American outflow	25–45° N	85–70° W	40.3 ± 4.7	-0.8 ± 0.4
C. Southern Europe	35–50° N	1–25° E	41.6 ± 4.3	-0.9 ± 0.5
D. Siberia	**50–65° N**	**50–80° E**	39.3 ± 6.5	-1.8 ± 0.5
E. Northern South America	**10–0° S**	**80–65° W**	25.4 ± 4.9	-1.6 ± 0.5
F. Southern South America	**40–20° S**	**75–45° W**	28.6 ± 4.7	1.2 ± 0.3
G. Southern Africa	**15–5° S**	**25–35° E**	27.6 ± 5.3	1.6 ± 0.5
H. Southeast Asia	**15–35° N**	**80–115° E**	34.6 ± 5.1	1.9 ± 0.5
I. North Australia outflow	**20–10° S**	**100–130° E**	26.8 ± 4.4	1.2 ± 0.4
J. Galapagos Islands	10° S–5° N	105–85° W	27.7 ± 5.2	-0.7 ± 0.5
I. Southern Pacific Ocean	70–30° S	120–75° W	25.4 ± 3.7	-0.4 ± 0.3

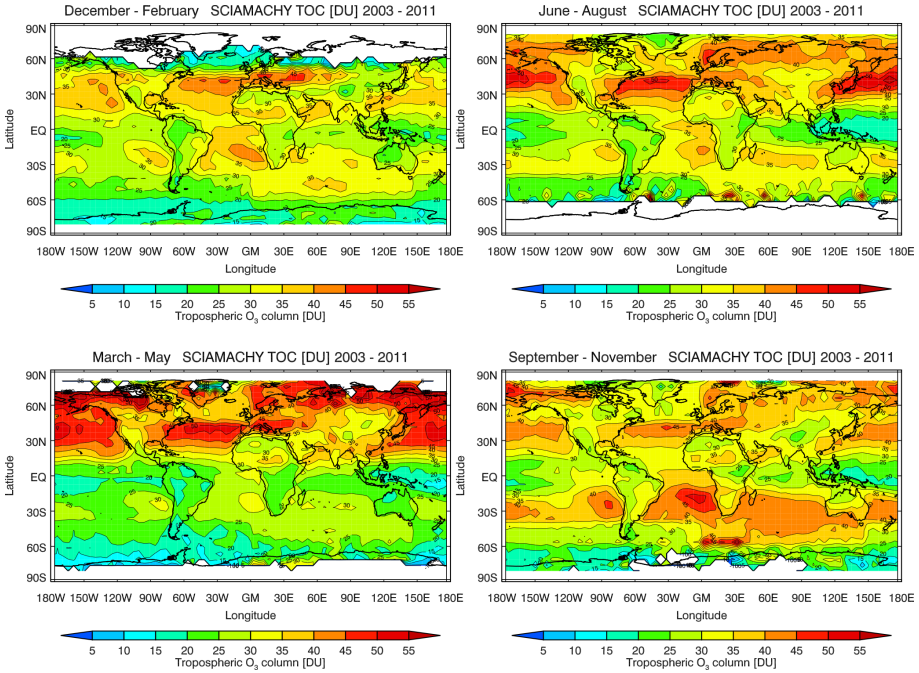

Figure 1. Global distribution of the seasonal tropospheric O_3 in DU from 2003–2011 for 5° latitude × 5° longitude bins. For latitudes above about 60° in each hemisphere O_3 columns are only observed during summer.

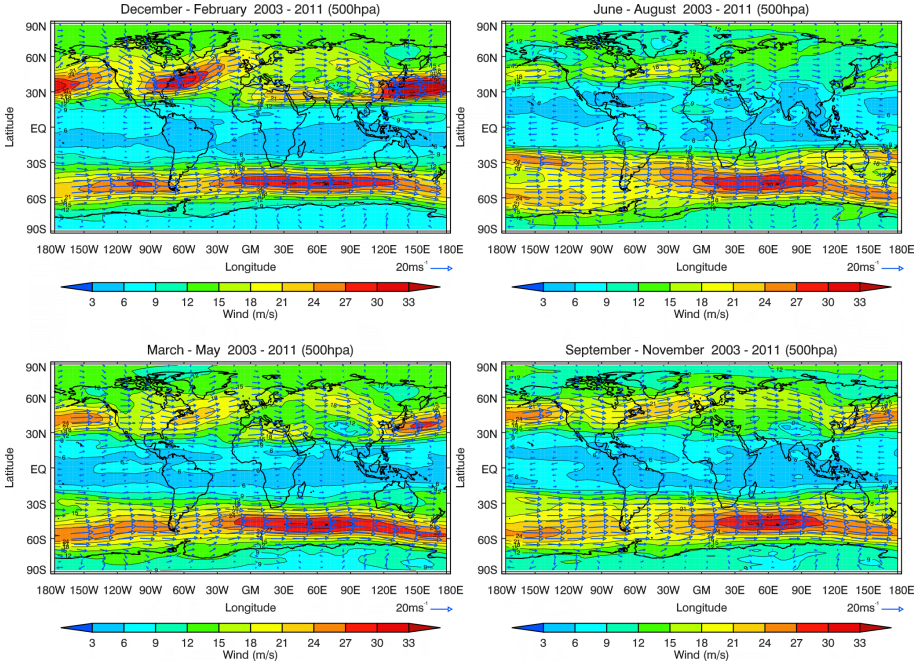

Figure 2. Global distribution of the seasonal winds at the 500 hPa pressure level from the ECMWF (European Centre for Medium-Range Weather Forecasts) from 2003–2011 for 5° latitude × 10° longitude bins.

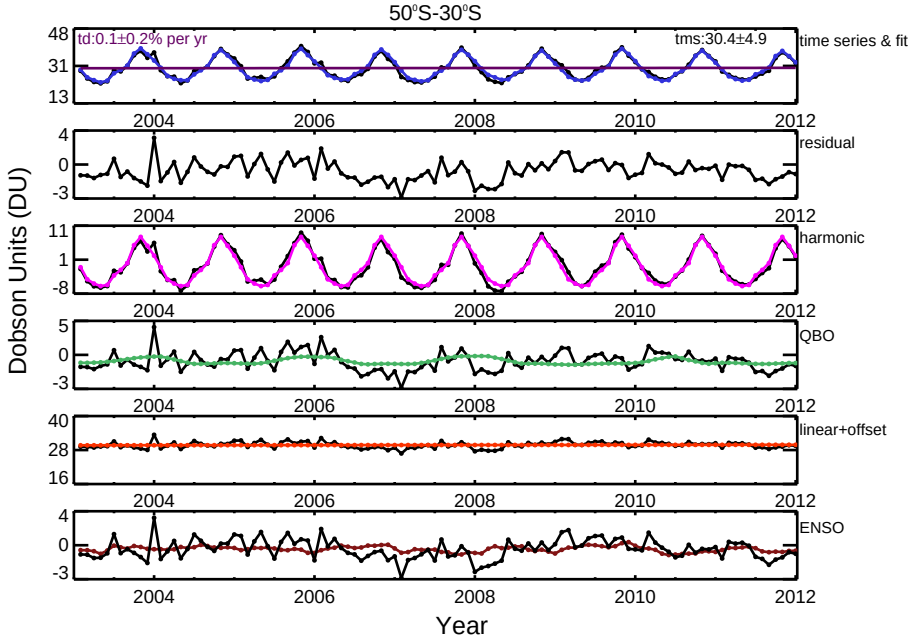

Figure 3. Time series (in Dobson Units (DU)) from SCIAMACHY for 50–30° S (black) with overlaid fitting curve (blue in top panel) and fit residuals (second panel). Below, the components of the linear regression are shown individually (from top to bottom): harmonic (pink), QBO (light green), linear change (orange), and ENSO (brown). Each of these terms is overlaid by the time series with all other components of the fitting curve subtracted.

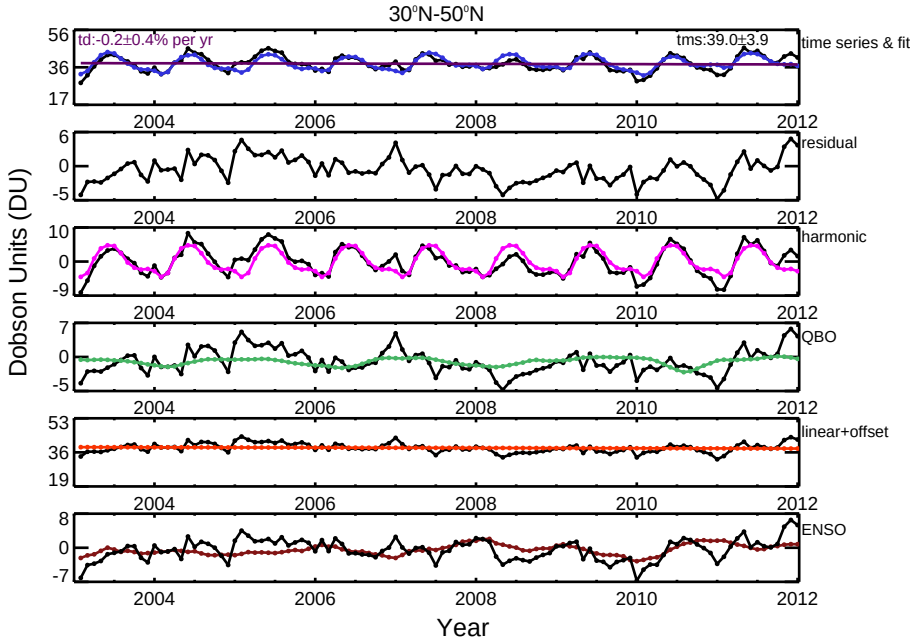

Figure 4. Same as Fig. 3 but for 30–50° N.

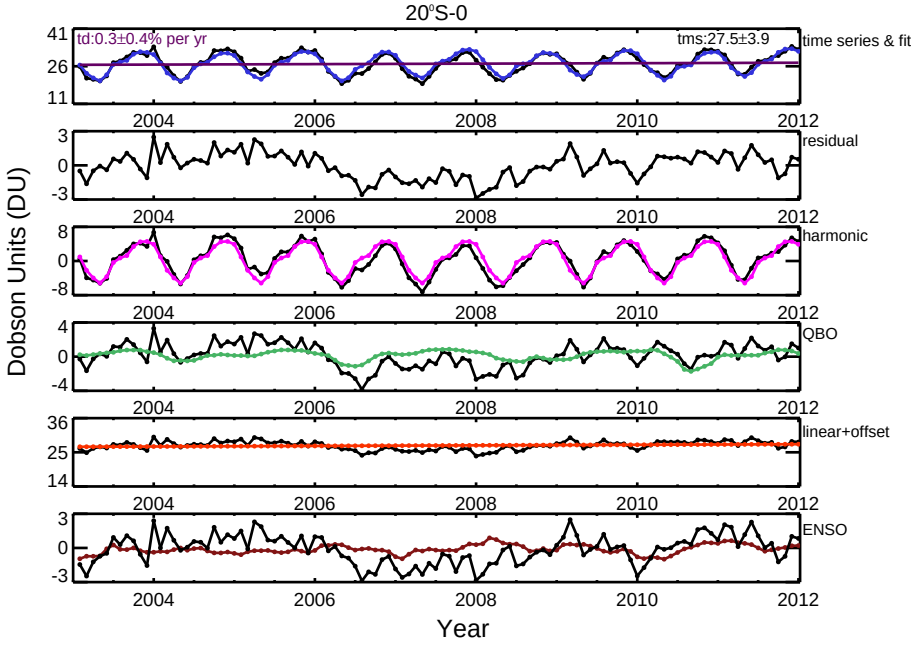

Figure 5. Same as Fig. 3 but for 20° S–0.

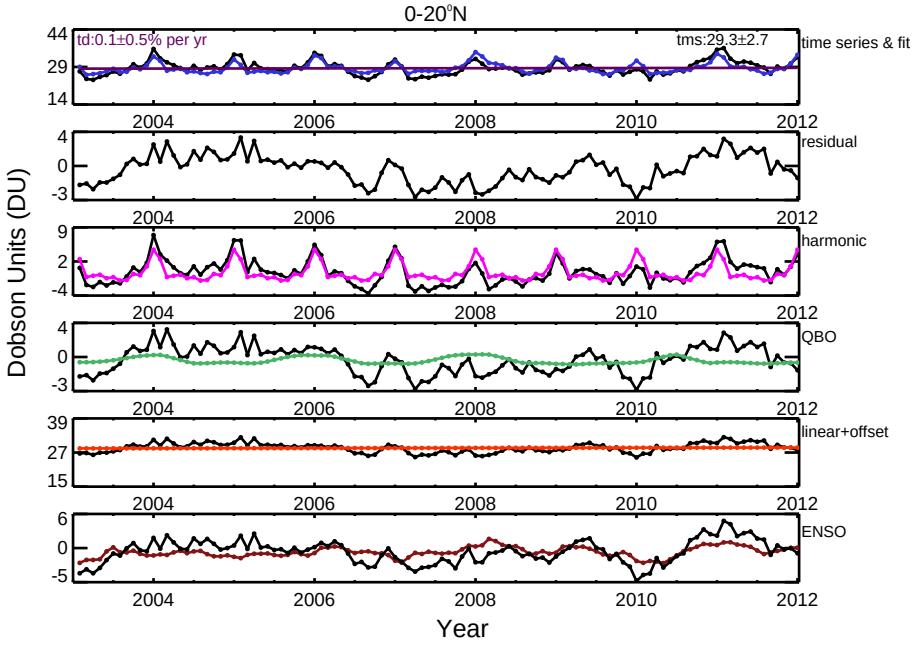

Figure 6. Same as Fig. 3 but for 0–20° N.

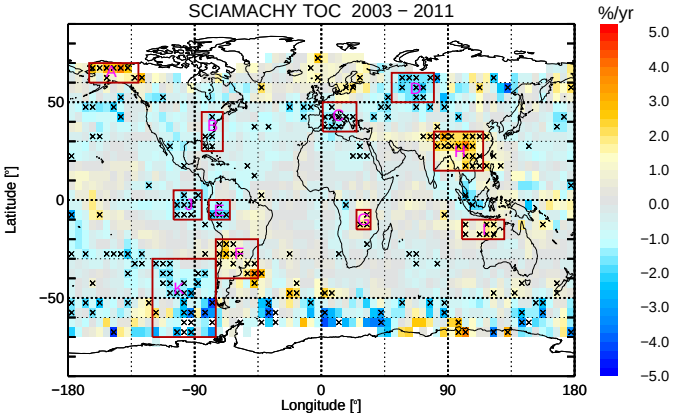

Figure 7. Changes in SCIAMACHY tropospheric O_3 columns ($\%\,yr^{-1}$) derived for the period 2003–2011 with 5° latitude × 5° longitude resolution. The regions with cross signs describe statistically significant change and the white coloured areas represent places with no trend data.

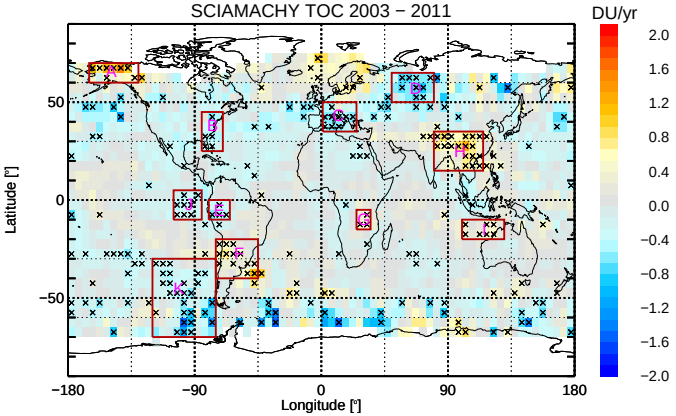

Figure 8. Changes in SCIAMACHY tropospheric O_3 columns (DU/yr) derived for the period 2003–2011 with 5° latitude × 5° longitude resolution. The regions marked with crosses describe statistically significant trends and the white coloured areas represent places with no trend data.

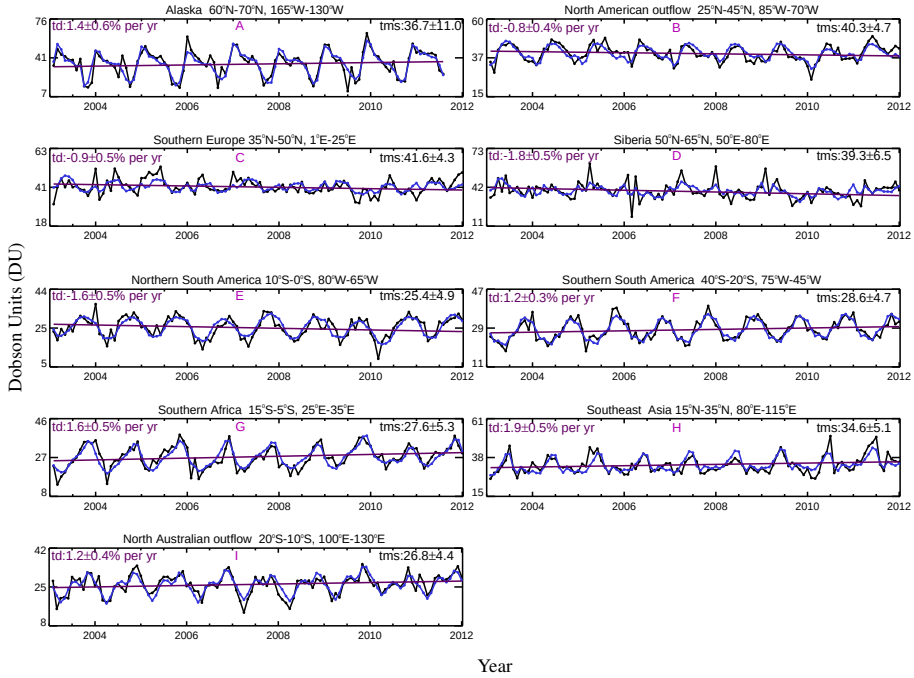

Figure 9. Time series (in Dobson Units (DU)) (black) from SCIAMACHY (for the different regions A–I shown in Fig. 7) with overlaid fitting curves (blue) and linear change plus offset (violet) for the years 2003–2011.